ZnO nanocoral structures for photoelectrochemical cells

Kwang-Soon Ahn,[a] Yanfa Yan, Sudhakar Shet, Kim Jones, Todd Deutsch, John Turner, and Mowafak Al-Jassim
National Renewable Energy Laboratory, Golden, Colorado 80401, USA

(Received 20 August 2008; accepted 28 September 2008; published online 24 October 2008)

We report on synthesis of a uniform and large area of a new form of ZnO nanocorals. These nanostructures can provide suitable electrical pathways for efficient carrier collection as well as large surface areas for the photoelectrochemical (PEC) cells. PEC devices made from these ZnO nanocoral structures demonstrate significantly enhanced photoresponse as compared to ZnO compact and nanorod films. Our results suggest that the nanocoral structures could be an excellent choice for nanomaterial-based applications such as dye-sensitized solar cells, electrochromic windows, and batteries. © *2008 American Institute of Physics*. [DOI: 10.1063/1.3002282]

Nanostructured materials can offer significant advantages for applications of key technologies such as photoelectrochemical (PEC) energy conversion for hydrogen production, dye-sensitized solar cells, Li ion batteries, electrochromic windows, and catalysts, due to their large surface areas.[1–9] The form, orientation, and contact of the nanostructures can dramatically affect the transport properties and therefore can play a critical role in the performance of these devices.[3,4,10,11] It is thus important to find the appropriate nanostructures to achieve the best characteristics for device performance. Here, we report on synthesis of a uniform and large area of a new form of ZnO nanostructures, which we term ZnO nanocorals. These nanostructures can provide large surface areas and suitable electrical pathways for efficient carrier collection. PEC devices made from these ZnO nanocoral structures demonstrate significantly enhanced photoresponse as compared to compact and other nanostructure ZnO films. Our results suggest that the nanocoral structures could be an excellent choice for other nanomaterial-based applications such as dye-sensitized solar cells, electrochromic windows, and batteries.

PEC systems based on transition metal oxides, such as TiO_2, Fe_2O_3, ZnO, and WO_3, have received extensive attention since the discovery of the photo-induced decomposition of water on TiO_2 electrodes.[3,8,9,12] Nanostructures of these materials are often used to enhance the efficiency of these materials due to the increased surface area. Among these oxides, ZnO is known to be the material that will most easily form nanostructures.[13–17] We have found that aligned ZnO nanorods can indeed improve PEC performance as compared to compact ZnO films grown under similar conditions.[18] However, the enhancement gained from the aligned nanorods is significantly less than the enhancement realized by the nanocorals.

ZnO nanocoral structures were synthesized by a two-step process: the deposition of Zn metal thin films followed by thermal oxidation at 500 °C in a quartz tube furnace with flowing O_2. Zn metal films were grown by rf magnetron sputtering. *F*-doped SnO_2 fluorine tin oxide (FTO), (8–10 Ω/□)-coated transparent glasses (TEC-8) were used as substrates for PEC applications. The substrates were rotated and the distance between the metallic Zn target (3 in. diameter) and the substrate was 8 cm. The working pressure was 1.1×10^{-2}Torr under Ar ambient. Sputtering was conducted at room temperature at rf powers of 35, 50, 100, 150, and 200 W. All samples have a similar film thickness of about 1.4 μm as measured by stylus profilometry. After deposition, the Zn films were vacuum sealed and kept in the N_2 desiccators to eliminate surface oxidization. ZnO nanostructures were formed by postannealing the Zn films at 500 °C for 8 h with the O_2 flowing [40 SCCM (SCCM denotes cubic centimeter per minute at STP)] in a three-zone quartz tube furnace.

PEC measurements were performed in a three-electrode cell with a flat quartz window.[18,19] The ZnO films (area: 0.24 cm^2) were used as the working electrodes. A Pt sheet (area: 10 cm^2) and a Ag/AgCl (with saturated KCl) were used as counter and reference electrodes, respectively. A 0.5*M* Na_2SO_4 aqueous solution with a *p*H of 6.8 was used as the electrolyte for the stability of the ZnO.[18,19] The PEC response was measured using a fiber-optic illuminator (tungsten-halogen lamp) with a UV/IR cutoff filter (cutoff wavelengths: 350 and 750 nm). Light intensity with a UV/IR filter was 125 mW/cm^2. The PEC response under chopped illumination was measured during a potential sweep at a scan rate=5 mV/s.

The rf power was observed to have a great influence over the grain size and orientation of the synthesized Zn metal films and ultimately the microstructure of the thermally oxidized ZnO films. A set of Zn films were synthesized under the same growth conditions except with a variation in rf powers of 35, 50, 100, 150, and 200 W. After thermal oxidization, only those samples deposited with rf powers of 50 and 100 W exhibited the nanocoral structure.

The effect of rf power on the grain size and orientation of the synthesized Zn films is revealed using x-ray diffraction (XRD) curves shown in Fig. 1(a). The sputtering was performed under Ar ambient, so all samples exhibited pure Zn metal phases. The peak intensity and the full width at half maximum show that the grain size increases with the increasing rf power. This is due to the increased energy of the sputtered Zn ions.[20,21] It is evident that the intensity of the (0002) peak increases with the increasing rf power. Figure 1(b) shows the intensity ratio between the (0002) and the $(10\bar{1}1)$ peaks for the Zn films as a function of the rf power. The intensity ratio is 0.53 for Zn powder samples. It is seen that

[a]Electronic mail: kwang-soon_ahn@nrel.gov. Tel.: 1-303-384-6469.

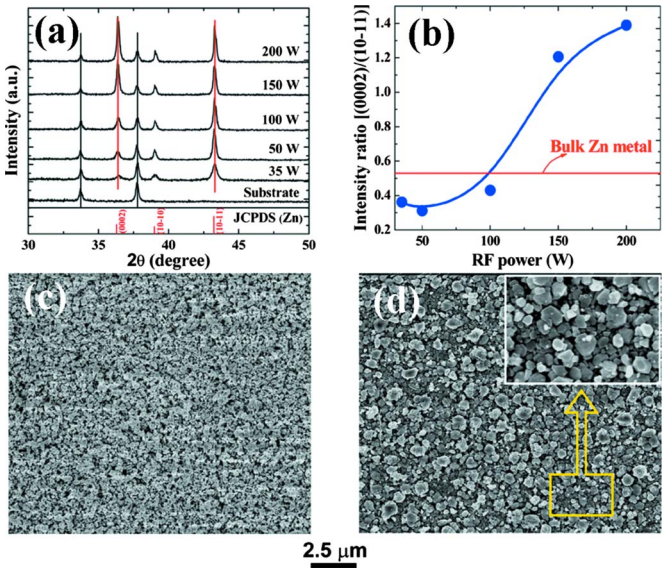

FIG. 1. (Color online) (a) XRD curves of the Zn metal films deposited at rf powers of 35, 50, 100, 150, and 200 W. (b) XRD peak intensity ratio of $(0002)/(10\bar{1}1)$ estimated from (a). [(c) and (d)] SEM images of 50 and 200 W-Zn films, respectively.

the Zn films deposited at rf powers higher than 150 W exhibited a higher peak intensity ratio, indicating that high rf power promotes (0002) orientation. Figures 1(c) and 1(d) show the scanning electron microscopy (SEM) images for the Zn films deposited at 50 and 200 W, respectively. It shows clearly that the Zn film deposited at 50 W has randomly oriented small grains, whereas the 200 W- Zn film exhibited large hexagonlike grains. This is in a good agreement with the XRD results.

The annealed samples were named as 35, 50, 100, 150, and 200 W-ZnO. Figure 2 shows the SEM images taken from the annealed samples of 35, 50, 100, and 150 W-ZnO, respectively. Clearly the 50 W-ZnO [Fig. 1(b)] and the 100 W-ZnO [Fig. 1(c)] samples exhibit a nanocoral structure. The average size of the nanocorals for the 50 W-ZnO is significantly smaller than that for the 100 W-ZnO sample, indicating that the size of the nanocorals can be tuned by the rf power. The 35 W-ZnO consists of nanoparticles [Fig. 2(a)].

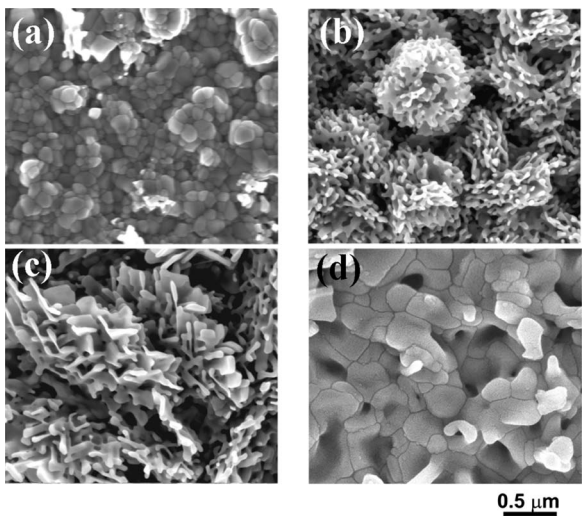

FIG. 2. Microstructures of thermal oxidized ZnO films. [(a)–(d)] SEM images of 35, 50, 100, and 150 W-ZnO films.

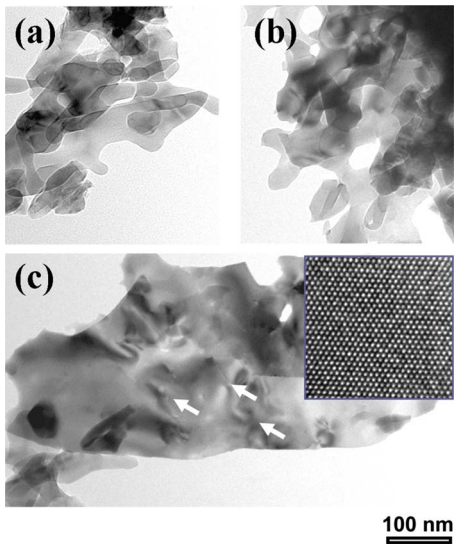

FIG. 3. (Color online) TEM images of the nanocoral structures. [(a) and (b)] Typical BF TEM images taken from 50 and 100 W-ZnO. (c) Typical large-size nanosheets. The inset is a HRTEM image from a nanosheet in sample 100 W-ZnO.

The 150 W-ZnO and the 200 W-ZnO (SEM image not shown here) are just nanocrystalline ZnO films [Fig. 1(d)]. We note that these nanoparticle and nanocrystalline films are not as compact as films directly deposited as ZnO. The SEM images reveal two unique features for the nanocoral structures. First, because the nanocorals are composed of nanosheets, the structure is very porous, producing a large surface area. Because of no sufficient powders from these thin films, estimation on the absolute surface areas cannot be made. However, the qualitative estimation can be drawn from SEM images. Second, the nanosheets grow together smoothly, providing an excellent electrical pathway for carrier collection. These two unique features are very favorable for PEC applications.[3,9,22,23]

The nanosheet features in the nanocoral nanostructures were further examined using transmission electron microscopy (TEM). Figures 3(a) and 3(b) show bright-field (BF) TEM images taken from samples 50 and 100 W-ZnO, respectively. The nanosheet features are clearly evident. We found that the sizes of nanosheets in sample 50 W-ZnO are more uniform than that in the sample of 100 W-ZnO. The nanosheets in sample 50 W-ZnO are typically similar to those shown in Fig. 3(a). However, in the sample of 100 W-ZnO, additional nanosheets with much larger sizes than those seen in Fig. 3(b) are often observed. Figure 3(c) shows an example of a large nanosheet seen in the sample of 100 W-ZnO. From the diffraction contrast, we also observed that the nanosheets are typically single crystals. The nanosheets with small sizes are usually free from lattice defects and strains, while the nanosheets with large sizes usually contain defects and strains, marked by the white arrows in Fig. 3(c). We have further determined that the growth direction of the nanosheets is the nonpolar surface of $(11\bar{2}0)$. The inset in Fig. 3(c) shows a high-resolution TEM image (HRTEM) taken from a nanosheet.

The above SEM and TEM images show that the sample 50 W-ZnO has smaller nanosheets, larger surface area, and better crystallinity than the sample 100 W-ZnO. Thus, the 50 W-ZnO is expected to exhibit better PEC performance than

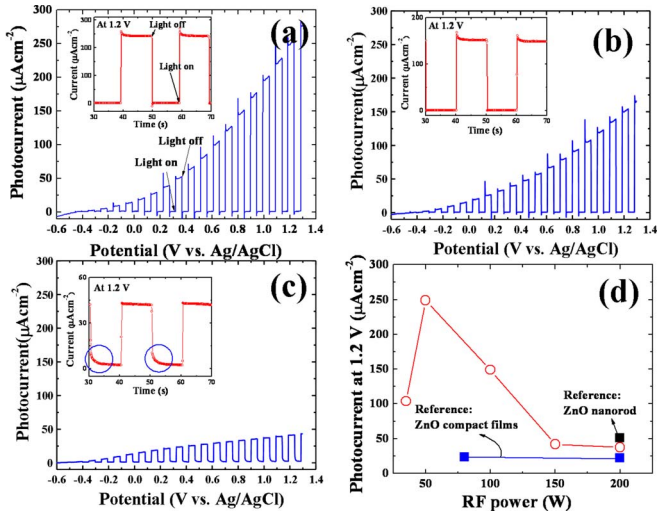

FIG. 4. (Color online) [(a)–(c)] Photocurrent-voltage curves of the 50, 100, and 150 W-ZnO nanostructural films, respectively, measured under chopped illumination with an UV/IR cutoff filter. Insets are the current transient with time performed at 1.2 V under the light on/off illumination. (d) Photocurrents of different ZnO films measured at 1.2 V.

100 W-ZnO. Figures 4(a)–4(c) show the photocurrent-voltage curves for the 50, 100, and 150 W-ZnO films, respectively, under chopped light illumination with an UV/IR filter. To compare the PEC responses, the photocurrents for all samples at 1.2 V were plotted [Fig. 4(d)]. For comparison, the PEC responses of ZnO compact and nanorod films reported elsewhere[18,19] are also plotted in Fig. 4(c). Because all the films have similar thicknesses, the photocurrents can be compared. Clearly, the nanoparticle film (35 W-ZnO) and the nanocoral films (50 and 100 W-ZnO) exhibited higher PEC responses than compact and nanorod films. Among them, the 50 W-ZnO nanocoral film exhibited the best PEC response and its photocurrent at 1.2 V is ten and five times higher than those of the compact and nanorod films. On the other hand, the 150 and 200 W-ZnO films showed much lower PEC responses than the ZnO coral nanostructures. The insets in Figs. 4(a)–4(c) show the current transients, performed at constant 1.2 V under light on/off illumination. The photocurrents of the ZnO nanocoral structures decay very sharply without exhibiting photocurrent tails under light-off conditions. However, the photocurrents for the nanocrystalline ZnO structures (150 W-ZnO) decay slowly showing photocurrent tails, indicating a trap-related carrier transport process [see the circles in the inset of Fig. 4(c)].[4,23–25] This suggests that the ZnO nanocoral films have much better carrier transport than the nanocrystalline structures. This can be attributed to the deformation-free nature and smooth electrical pathway as shown in the SEM and TEM results. The comparative PEC performance tests have been repeated many runs, and the results are reproducible.

In summary, we have synthesized porous ZnO nanocoral structures on FTO substrates using a two-step process. The nanocoral structure provides a large surface area, superior light trapping, and an excellent pathway for carrier transport. With our ZnO nanocoral films (50 W-ZnO), we have demonstrated a significantly enhanced PEC response as compared to compact and nanorod films. Thus, the nanocoral structure could be an interesting form for nanomaterial-based applications including catalysts, batteries, and electrochromism.

This work was supported by the U.S. Department of Energy through the UNLV Research Foundation.

[1] *Zinc Oxide Bulk, Thin Films and Nanostructures*, edited by C. P. Jagadish (Elsevier, Oxford, 2006).
[2] B. O'Regan and M. Gratzel, Nature (London) **353**, 737 (1991).
[3] C. M. Lopez and K. S. Choi, Chem. Commun. (Cambridge) **2005** 3328.
[4] M. Law, L. E. Greene, J. C. Johnson, R. Saykally, and P. D. Yang, Nature Mater. **4**, 455 (2005).
[5] W. I. Park, D. H. Kim, S. W. Jung, and G. C. Yi, Appl. Phys. Lett. **80**, 4232 (2002).
[6] S. H. Lee, R. Deshpande, P. A. Parilla, K. M. Jones, B. To, A. H. Mahan, and A. C. Dillon, Adv. Mater. (Weinheim, Ger.) **18**, 763 (2006).
[7] S. H. Kang, J. Y. Kim, Y. Kim, H. S. Kim, and Y. E. Sung, J. Phys. Chem. C **111**, 9614 (2007).
[8] A. Fujishima and K. Honda, Nature (London) **238**, 37 (1972).
[9] T. F. Jaramillo, S. H. Baeck, A. Kleiman-Shwarsctein, and E. W. McFarland, Macromol. Rapid Commun. **25**, 297 (2004).
[10] C. Santato, M. Ulmann, and J. Augustynski, Adv. Mater. (Weinheim, Ger.) **13**, 511 (2001).
[11] R. Beranek, H. Tsuchiya, T. Sugishima, J. M. Macak, L. Taveira, S. Fujimoto, H. Kisch, and P. Schmuki, Appl. Phys. Lett. **87**, 243114 (2005).
[12] D. Paluselli, B. Marsen, E. L. Miller, and R. E. Rocheleau, Electrochem. Solid-State Lett. **8**, G301 (2005).
[13] H. Y. Dang, J. Wang, and S. S. Fan, Nanotechnology **14**, 738 (2003).
[14] X. Y. Kong and Z. L. Wang, Nano Lett. **3**, 1625 (2003).
[15] Z. R. R. Tian, J. A. Voigt, J. Liu, B. McKenzie, M. J. McDermott, M. A. Rodriguez, H. Konishi, and H. F. Xu, Nature Mater. **2**, 821 (2003).
[16] H. J. Fan, R. Scholz, F. M. Kolb, and M. Zacharias, Appl. Phys. Lett. **85**, 4142 (2004).
[17] H. J. Fan, R. Scholz, F. M. Kolb, M. Zacharias, U. Gosele, F. Heyroth, C. Eisenschmidt, T. Hempel, and J. Christen, Appl. Phys. A: Mater. Sci. Process. **79**, 1895 (2004).
[18] K. S. Ahn, T. Deutsch, C. S. Jiang, Y. Yan, M. Al-Jassim, and J. Turner, J. Power Sources **176**, 387 (2008).
[19] K. S. Ahn, Y. Yan, S. H. Lee, T. Deutsch, J. Turner, C. E. Tracy, C. L. Perkins, and M. Al-Jassim, J. Electrochem. Soc. **154**, B956 (2007).
[20] Y. C. Choi, Y. M. Shin, Y. H. Lee, B. S. Lee, G. S. Park, W. B. Choi, N. S. Lee, and J. M. Kim, Appl. Phys. Lett. **76**, 2367 (2000).
[21] K. S. Ahn, Y. Yan, and M. Al-Jassim, J. Vac. Sci. Technol. B **25**, L23 (2007).
[22] K. Vinodgopal, S. Hotchandani, and P. V. Kamat, J. Phys. Chem. **97**, 9040 (1993).
[23] A. Ghicov, H. Tsuchiya, J. M. Macak, and P. Schmuki, Phys. Status Solidi A **203**, R28 (2006).
[24] S. Nakade, T. Kanzaki, Y. Wada, and S. Yanagida, Langmuir **21**, 10803 (2005).
[25] K. S. Ahn, M. S. Kang, J. K. Lee, B. C. Shin, and J. W. Lee, Appl. Phys. Lett. **89**, 013103 (2006).